New Phytologist

Antecedent soil water content and vapor pressure deficit interactively control water potential in *Larrea tridentata*

Jessica S. Guo[1,2] and **Kiona Ogle**[1,2,3]

[1]Department of Biological Sciences, Northern Arizona University, Flagstaff, AZ 86011, USA; [2]The Center for Ecosystem Science and Society, Northern Arizona University, Flagstaff, AZ 86011, USA; [3]School of Informatics, Computing, and Cyber Systems, Northern Arizona University, Flagstaff, AZ 86011, USA

Author for correspondence:
Jessica S. Guo
Tel: +1 928 523 0101
Email: jsg88@nau.edu

Received: *22 December 2017*
Accepted: *4 July 2018*

New Phytologist (2019) **221:** 218–232
doi: 10.1111/nph.15374

Key words: antecedent conditions, atmospheric drought, hysteresis, *Larrea tridentata* (creosotebush), soil moisture, stomatal regulation, temporal lags, water potential.

Summary

- Plant water potential Ψ is regulated by stomatal responses to atmospheric moisture demand *D* and soil water availability *W*, but the timescales of influence and interactions between these drivers of plant Ψ are poorly understood.
- Here, we quantify the effects of antecedent *D* and *W* on plant Ψ in the desert shrub *Larrea tridentata.* Repeated measurements of plant baseline water potential Ψ_B and diurnal water potential Ψ_D were analyzed in a Bayesian framework to evaluate the influence of antecedent *D* and *W* at daily and subdaily timescales.
- Both Ψ_B and Ψ_D exhibited negative, 2- to 4-d lagged responses to daily-scale *D*; conversely, plant Ψ_D responded almost instantaneously to subdaily *D*, though the direction of this response depended on antecedent moisture conditions. Plant Ψ_B and Ψ_D responded positively and immediately (no lag) to shallow *W*, which contrasts the negative, lagged (6–7 d) response to deep *W*.
- The changing sensitivity of Ψ_D to subdaily *D* highlights shifting modes of plant Ψ regulation: *D* effects on Ψ_D range from negative to neutral to positive depending on past conditions and time of day. Explicit consideration of antecedent conditions across multiple timescales can reveal important complexities in plant responses.

Introduction

Water potential Ψ of a plant leaf or stem is an integrated measure of plant water status that interacts with critical functions such as stomatal conductance (Tardieu & Davies, 1992), hydraulic conductivity (Pockman & Sperry, 2000), sugar transport (Hölttä *et al.*, 2009), and whole-plant transpiration (Sperry *et al.*, 2002). Plant Ψ must be regulated above a critical threshold to prevent hydraulic failure (Sperry *et al.*, 2002), wherein xylem conduits are fully embolized and the plant can no longer supply its leaves with water (Brodribb & Cochard, 2009; Urli *et al.*, 2013). To maintain tissue hydration, plant Ψ is exogenously influenced by soil water content *W* and vapor pressure deficit *D* (Cowan, 1965; Jarvis, 1976) and endogenously regulated by stomatal responses to *W* and *D* (Jones & Sutherland, 1991; Cochard *et al.*, 1996). Regulation of plant Ψ can be interpreted in terms of iso-/anisohydric stomatal behavior (*sensu* Tardieu & Simonneau, 1998; and see Hochberg *et al.*, 2018 for a broader set of definitions): isohydric species maintain fairly constant plant Ψ due to strict stomatal control, whereas anisohydric species exhibit wider ranges of plant Ψ due to loose stomata regulation (Jones, 1998; Tardieu & Simonneau, 1998). However, plant responses and regulation may lag behind environmental stimuli, partly due to delays associated with plants sensing the stimuli and subsequently transporting the associated signal (Chaves *et al.*, 2009).

Though quantitative studies of plant hydraulic function often assume that physiological variables respond to environmental conditions in near real time (e.g. Jones & Sutherland, 1991; Oren *et al.*, 1999), physiological processes often depend on antecedent (past) conditions (Ogle *et al.*, 2015). For example, stomatal conductance can remain suppressed days to weeks after a watering event that breaks soil drought (Gallé & Feller, 2007; Flexas *et al.*, 2009; Xu *et al.*, 2009), possibly because the rate of water infiltration (Castillo *et al.*, 2003; Rigby & Porporato, 2006) and recovery of hydraulic conductance (Lo Gullo *et al.*, 1998; Blackman *et al.*, 2009) depend on antecedent *W*. More directly, stomatal sensitivity to *D* can depend on past *D* conditions (Barbour & Buckley, 2007), resulting in delayed shifts in rates of transpiration and carbon uptake (Goldstein *et al.*, 2000; Pfautsch & Adams, 2013). Stomatal and plant Ψ responsiveness to soil and atmospheric moisture are therefore not always immediate (BassiriRad *et al.*, 1999; Yan *et al.*, 2000; Resco *et al.*, 2008) and can occur on longer temporal scales than previously thought (Ogle *et al.*, 2015; Kropp *et al.*, 2017). Because cumulative effects of lagged plant responses have the potential to impact ecosystem-scale carbon and water fluxes (e.g. Anderegg *et al.*, 2015; Ryan *et al.*, 2015; Shen *et al.*, 2016; Kropp *et al.*, 2017; Schwalm *et al.*, 2017), it is important to quantify and understand the temporal lags in plant ecophysiological responses.

The evergreen desert shrub *Larrea tridentata* (creosote bush, referred to hereafter as *Larrea*) is the most abundant perennial plant of the North American warm deserts (Smith *et al.*, 1997). *Larrea* is remarkably drought tolerant and actively photosynthesizes despite high temperatures (Mooney *et al.*, 1978) and low Ψ (Franco *et al.*, 1994). Year-round maintenance of a hydrated canopy (Runyon, 1936) and positive carbon uptake (Oechel *et al.*, 1972; Odening *et al.*, 1974), even when predawn Ψ drops to or below −10 MPa (Cunningham & Burk, 1973), likely requires *Larrea* to employ a suite of physiological responses that integrate across variable current and antecedent conditions. Stomatal behavior in *Larrea* is expected to be relatively anisohydric (Ogle *et al.*, 2012), but *Larrea*'s stomata are nonetheless sensitive to high *D* and experience midday closure (Oechel *et al.*, 1972; Franco *et al.*, 1994). Recent work suggests that stomatal behavior along the iso-/anisohydric spectrum may vary depending on environmental conditions (Hochberg *et al.*, 2018), highlighting the possible importance of antecedent conditions for regulation of plant Ψ. Particularly at longer (e.g. seasonal) timescales, tight regulation of plant Ψ is not necessarily attributable to greater stomatal control (Martínez-Vilalta & Garcia-Forner, 2017); conversely, very low plant Ψ can be associated with strict stomatal control (Garcia-Forner *et al.*, 2016). Rather than study multiple metrics of iso-/anisohydry (Berger-Landefeldt, 1936; Tardieu & Simonneau, 1998; Klein, 2014; Martínez-Vilalta *et al.*, 2014; Skelton *et al.*, 2015; Hochberg *et al.*, 2018), we focused on the sensitivity of plant Ψ to antecedent environmental drivers. As a dominant warm desert plant with documented temporal lags in stomatal conductance (Ogle *et al.*, 2015), *Larrea* is an appropriate study organism to investigate the effect of antecedent conditions on plant Ψ and the potential implications for stomatal regulation of plant Ψ.

In this study, we evaluate plant Ψ dynamics in the context of baseline (predawn and early morning) water potential Ψ_B values, which anchor the within-day variation described by diurnal water potential Ψ_D. We expect Ψ_B and Ψ_D to respond to environmental drivers on different temporal scales. Predawn Ψ is measured before the start of daily photosynthesis, generally represents the maximum daily plant Ψ, and is expected to reflect soil Ψ due to potential overnight equilibration between the plant and soil. However, disequilibrium between predawn plant Ψ and soil Ψ has been observed in multiple species under well-watered conditions (Donovan *et al.*, 2001), possibly attributable to nocturnal transpiration (Donovan *et al.*, 2003; Bucci *et al.*, 2005), which can be up to 25% of daytime transpiration in *Larrea* (Ogle *et al.*, 2012). Therefore, predawn Ψ could depend not only on soil Ψ but also on antecedent atmospheric conditions (e.g. *D*) that affect nocturnal transpiration rates (Sellin, 1999; Barbour & Buckley, 2007; Fisher *et al.*, 2007; Ogle *et al.*, 2012). Diurnal variation in Ψ is generally more negative than predawn Ψ, given higher daytime transpiration rates (Caird *et al.*, 2007; Forster, 2014). Since stomata typically respond to *D* on the order of minutes to hours (Damour *et al.*, 2010), subdaily changes in diurnal Ψ are likely closely linked to subdaily variation in *D*, but the sensitivity of diurnal Ψ to subdaily *D* and the timescales over which *D* affects diurnal Ψ are not clearly known.

Temporal patterns of plant responses may be particularly important in arid regions, as prolonged dry periods unsuitable for plant function are unpredictably interrupted by episodic precipitation (Noy-Meir, 1973; Loik *et al.*, 2004). Anticipated future conditions in the southwestern USA – higher temperatures, greater aridity, and lower soil moisture (Seager *et al.*, 2007; Garfin *et al.*, 2013; Prein *et al.*, 2016) – are expected to amplify plant water stress via extreme or prolonged episodes of low *W* and high *D* (Williams *et al.*, 2013). Consequently, more negative plant Ψ may lead to increased hydraulic dysfunction (Sperry *et al.*, 2002) and drought-induced mortality (McDowell *et al.*, 2013; Sperry & Love, 2015). Hence, clarifying the environmental conditions and associated timescales of influence that determine plant Ψ are important for predicting plant hydraulic responses under a changing climate. To address this challenge, we quantified the effects and timescales of influence (e.g. temporal lags) of antecedent *W* and *D* on plant Ψ_B and Ψ_D in *Larrea* by addressing the following questions: (Q1) How do soil and atmospheric moisture conditions control plant Ψ? (Q2) Over what timescales do these environmental drivers influence plant Ψ? (Q3) How might antecedent conditions impact regulation of plant Ψ in response to subdaily variation in atmospheric conditions (D)? We address these questions by analyzing repeated (within a day and across the growing season) observations of plant Ψ_B and Ψ_D in the context of the stochastic antecedent modeling (SAM) framework (Ogle *et al.*, 2015). This study is novel because we explicitly quantify the temporal lags in plant Ψ responses to soil and atmospheric moisture (*W* and *D*) by exploiting the variable moisture conditions of an arid system and drawing upon the SAM analysis approach.

Materials and Methods

Site description and data collection

From June 1998 to July 1999, 16 mature individuals of *L. tridentata* [DC] Cov. were selected for study at the Jornada Long-Term Ecological Research site in New Mexico, USA (described in Ogle & Reynolds, 2002). All shrubs occurred in a fenced enclosure and were within 20 m of a micrometeorological station and a centralized data collection and sensor operation system. Eight control shrubs were randomly selected to receive only ambient rainfall, wherease the other eight treatment shrubs were watered twice in summer 1998 (30 and 40 mm) and once in early spring 1999 (45 mm) in addition to receiving ambient rainfall. Irrigation was supplied by a gravity-fed hose and watering tank and confined to a circular area that extended about 0.25 m beyond the canopy drip line of each shrub. In the context of this study, irrigated and control groups are simply used to create greater variation in soil moisture conditions.

During the study period, small terminal twigs were repeatedly excised from each shrub between 05:00 h and 20:30 h local time on each sampling day. Plants were sampled on 11 d during the summer of 1998 and 6 d during the spring and summer of 1999, spanning a range of *D* and *W* conditions (Supporting Information Fig. S1). Plant Ψ was measured on excised stems with a

Scholander-type pressure chamber (Scholander *et al.*, 1965) between two and 10 times per sampling day (total $n = 1036$), spanning a range of plant water stress (Fig. 1). Four control and four treatment shrubs were intensely sampled ($n \geq 109$ measurements per shrub); the remaining shrubs were infrequently sampled ($n \leq 20$ per shrub). For logistical reasons, only nine measurements were made before sunrise ('predawn'), so we deemed plant Ψ measured before or within 1 h of sunrise as Ψ_B ($n = 151$). The remaining measurements represent Ψ_D time-series ($n = 885$) and were completed before sunset (Fig. 1).

The plant Ψ measurements were paired with shrub-level soil water content W and site-level atmospheric vapor pressure deficit D (Notes S1). Time-domain reflectometry probes were placed under eight of the 16 shrubs to measure 30 min W at two depth intervals (0–30 and 30–60 cm). *Larrea* has a small fraction of active roots in the top 2 cm, and the bulk of its active root area is found between 20 and 45 cm (Ogle *et al.*, 2004). Mean daily volumetric W was determined by daily averages of the half-hourly values, yielding shallow (W_{30}, 0–30 cm) and deep (W_{60}, 30–60 cm) estimates of water availability. Noninstrumented shrubs were paired with treatment-level (control or watered) W_{30} and W_{60} daily means. The micrometeorological station provided half-hourly averages of air temperature and relative humidity, which were used to compute D (Monteith & Unsworth, 1990); maximum daily D (max D) was calculated as the daily maximum of the half-hourly values.

Model description

The relationship between plant Ψ and antecedent moisture conditions (Table 1) was analyzed in a hierarchical Bayesian framework (Clark, 2005; Gelman *et al.*, 2014) to evaluate temporal relationships (e.g. lags) between plant Ψ and environmental conditions. Plant Ψ_B and Ψ_D were modeled separately to independently estimate the effects and temporal lags of the shared antecedent covariates (Notes S2, S3). To define the likelihood of these data, observed Ψ values were assumed to be normally distributed, such that for observation i:

$$\begin{aligned}\Psi_{B,i} &\sim \mathrm{Normal}(\mu_{B,i}, \sigma_B^2) \\ \Psi_{D,i} &\sim \mathrm{Normal}(\mu_{D,i}, \sigma_D^2)\end{aligned} \qquad \text{Eqn 1}$$

where μ is the predicted plant Ψ and σ^2 describes the observation variance, both of which differ among Ψ_B and Ψ_D data, as indicated by the B and D subscripts. Next, we model μ_B and μ_D as linear combinations of antecedent covariates (denoted as X_j^{ant} for

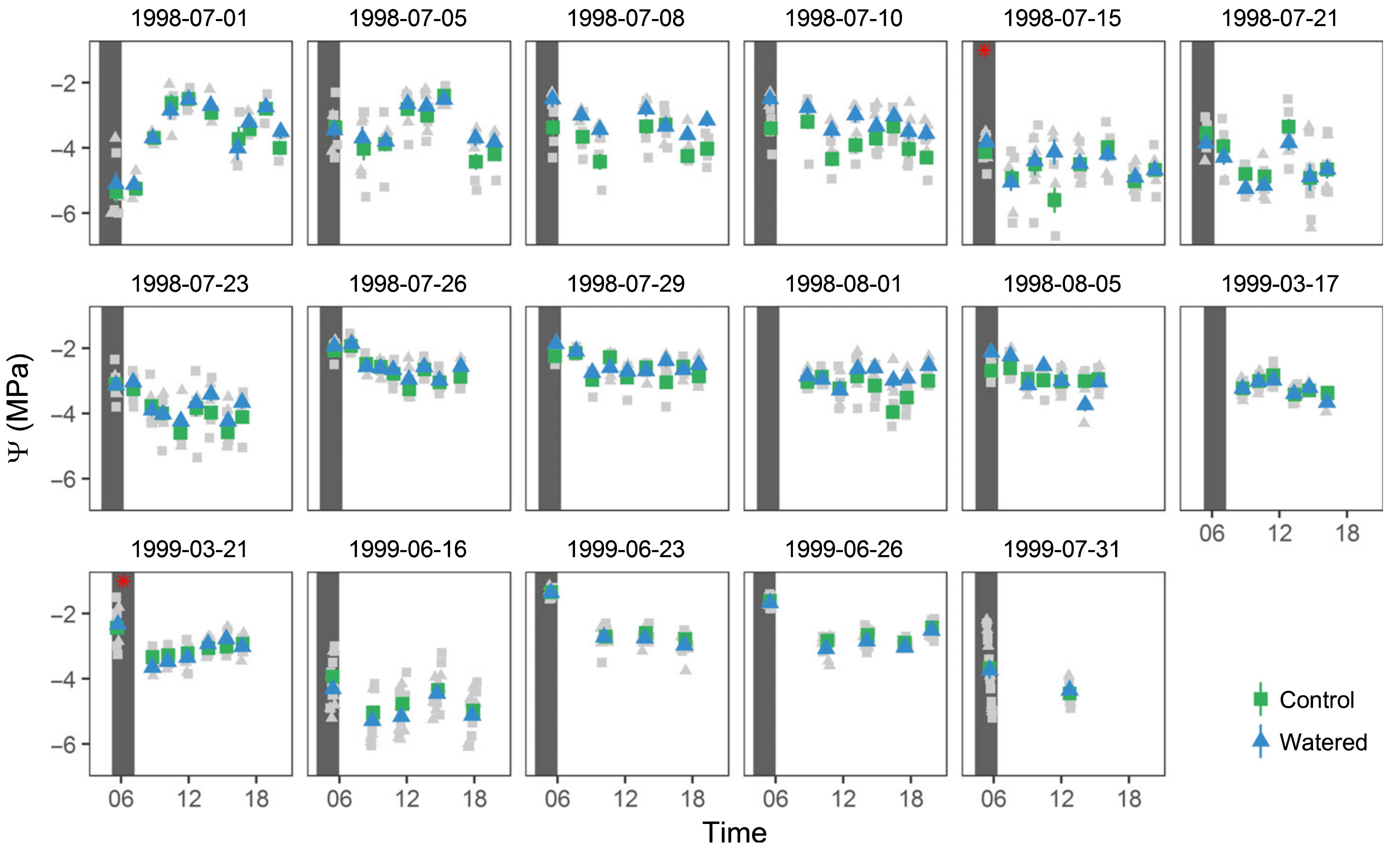

Fig. 1 Treatment-level plant water potential (Ψ) (mean ± SE) of control (green) and watered (blue) *Larrea tridentata* shrubs on 17 sampling days corresponding to the environmental conditions and sampling times indicated in Supporting Information Fig. S1. Plant Ψ of individual shrubs are in light gray. Vertical dark gray bars highlight sunrise ± 1 h; points occurring within the bar were considered baseline Ψ (Ψ_B), and all other measurements were considered diurnal Ψ (Ψ_D). Red asterisks indicate days where at least one Ψ value was measured before sunrise, indicating a true predawn value. Dates above panels are formatted as year–month–day.

Table 1 Notation used to denote antecedent covariates, their antecedent importance weights, the time-steps used to compute antecedent variables (Eqn 3), and the mean (nominal) values used to center the covariates in the baseline (Ψ_B) and diurnal (Ψ_D) water potential regressions (Eqn 2)

Symbolic variable*	Vectors of importance weights	Covariate	Definition	Units	Time step size, p	T_{lag}	Mean value
X_1^{ant}	ω_1	max D^{ant}	Daily maximum vapor pressure deficit	kPa	Daily	7	5
X_2^{ant}	ω_2	W_{30}^{ant}	Volumetric soil water content from 0 to 30 cm	$m^3\,m^{-3}$	Daily	7	10
X_3^{ant}	ω_3	W_{60}^{ant}	Volumetric soil water content from 30 to 60 cm	$m^3\,m^{-3}$	Daily	7	13
X_4^{ant}	ω_4	D^{ant}	Vapor pressure deficit D	kPa	Half-hourly	7	3
X_5^{ant}	ω_5	ΔD^{ant}	Change in D relative to previous value	kPa	Half-hourly	7	0

Weight vectors ω_1, ω_2 and ω_3 were estimated separately for the Ψ_B and Ψ_D models, and weight vectors ω_4 and ω_5 only apply to the Ψ_D model.
*Superscript 'ant' denotes the antecedent version of the covariate.

covariate j), including antecedent daily maximum D (max D), daily W_{30}, and daily W_{60} (μ_B and μ_D), and antecedent half-hourly D and change in D (ΔD; μ_D only), and all two-way interactions (see Table 1 for a list of covariates):

$$\mu_{B,i} = \beta_{0,s(i)} + \sum_{j=1}^{3} \beta_{j,s(i)} \cdot X^{ant}_{j,t(i)} + \sum_{j=1}^{3} \sum_{k=j+1}^{3} \beta_{jk,s(i)} \cdot X^{ant}_{j,t(i)} \cdot X^{ant}_{k,t(i)}$$

$$\mu_{D,i} = \alpha_{0,s(i)} + \sum_{j=1}^{5} \alpha_{j,s(i)} \cdot X^{ant}_{j,t(i)} + \sum_{j=1}^{5} \sum_{k=j+1}^{5} \alpha_{jk,s(i)} \cdot X^{ant}_{j,t(i)} \cdot X^{ant}_{k,t(i)}$$

Eqn 2

The β and α parameters were allowed to vary by shrub, akin to a random coefficients model, where $s(i)$ indicates shrub s associated with observation i. The antecedent covariates are continuous in time, and t indicates the specific time associated with observation i. The shrub-level main effects of covariate j on Ψ_B and Ψ_D are denoted by β_j and α_j respectively, and β_{jk} and α_{jk} indicate the interaction effects for covariates j and k ($j \neq k$). Antecedent covariates were centered near their mean values so that the intercepts (β_0 and α_0) are interpreted as the predicted shrub-level Ψ_B and Ψ_D respectively at 'nominal' environmental conditions (see Table 1 for the nominal values).

While we expect plant Ψ to respond to antecedent conditions, the relative importance of environmental drivers at different times into the past is not known *a priori*. Thus, to complete the specification of the mean model (Eqn 2), we employed the SAM approach (Ogle *et al.*, 2015) to simultaneously estimate the magnitude of the covariate effects and the timescale over which each variable influences plant Ψ_B and Ψ_D. Antecedent variables were constructed using continuous time-series of each covariate X_j such that:

$$X^{ant}_{j,t} = \sum_{p=1}^{T_{lag}} \omega_{j,p} \cdot X_{j,t-p} \qquad \text{Eqn 3}$$

where j indicates the identity of the covariate (Table 1), t indicates the time period, T_{lag} indicates the total number of past time periods to sum over, $\omega_{j,p}$ represents the weight or relative importance of the p^{th} time step into the past, and $X_{j,t-p}$ is the observed value of variable j at p time steps ago. Antecedent variable $X^{ant}_{j,t}$ is thus a weighted average of past X_j values, where the weights $\omega_{j,p}$ are determined stochastically by the data. Variation in $\omega_{j,p}$ with respect to past time period p reveals the temporal pattern of the relationship between plant Ψ and variable X_j. Because Ψ_B measurements were made within 1 h of sunrise, we used the previous day's daily-scale variables ($p = 1$) to represent 'current' conditions for both the Ψ_B and Ψ_D models.

To complete the Bayesian model, we specified priors for the unknown parameters, including hierarchical priors for the shrub-level main effects and interaction terms (see Eqn 2):

$$\beta_{j,s} \sim \text{Normal}(\mu_{\beta_j}, \sigma^2_{\beta_j}), j = 0, \ldots, 3$$
$$\beta_{jk,s} \sim \text{Normal}(\mu_{\beta_{jk}}, \sigma^2_{\beta_{jk}}), j = 1, \ldots, 3, k = j+1, \ldots, 3$$

Eqn 4a

$$\alpha_{j,s} \sim \text{Normal}(\mu_{\alpha_j}, \sigma^2_{\alpha_j}), j = 0, \ldots, 5$$
$$\alpha_{jk,s} \sim \text{Normal}(\mu_{\alpha_{jk}}, \sigma^2_{\alpha_{jk}}), j = 1, \ldots, 5, k = j+1, \ldots, 5$$

Eqn 4b

We assigned relatively noninformative, standard priors to all remaining parameters, including the population-level means (μ_α and μ_β terms), all variance-related terms (e.g. σ_α, σ_β, σ_B and σ_D), and the antecedent importance weights (ω_j vectors). Only the population-level intercept for the Ψ_D model ($\mu_{\alpha 0}$) was given a semi-informative prior, Uniform(-16, 0), because plant Ψ at mean environmental conditions is unlikely to exceed these bounds (Maherali *et al.*, 2004; Choat *et al.*, 2012; Larter *et al.*, 2015). See Methods S1 for a complete description of the priors.

Model interpretation and implementation

Eqns (1)–(4b) were combined to produce posterior distributions for all parameters of interest (e.g. covariate effects and antecedent importance weights), which are summarized by their posterior means and 95% central credible intervals (CIs) defined by the 2.5 and 97.5 percentiles of the posterior. In addition to the shrub- and population-level regression coefficients (covariate effects), we also computed treatment-level effects by averaging shrub-level parameters across shrubs within each treatment group (control vs watered), producing a posterior distribution for these quantities. An effect is deemed significant if its 95% CI does not overlap zero, indicating that the associated environmental variable or interaction term was important for determining plant Ψ.

We also quantified the sensitivity of Ψ_D to subdaily D ($S_{\Psi,D} = d\Psi_D/dD^{ant}$), which describes the degree to which Ψ_D changes for a unit change in D. We computed $S_{\Psi,D}$ for different combinations of max D^{ant} and W_{30}^{ant}, at three levels of ΔD^{ant} representing, roughly, morning ($\Delta D^{ant} > 0$), midday ($\Delta D^{ant} = 0$), and afternoon ($\Delta D^{ant} < 0$). Negative values of $S_{\Psi,D}$ indicate a drop in Ψ_D with increasing D, implying weak stomatal regulation. Values of $S_{\Psi,D}$ not significantly different from zero indicate no change in Ψ_D in response to changing D, implying strong stomatal regulation. Finally, positive values of $S_{\Psi,D}$ indicate increasing Ψ_D with increasing D, implying excessive stomatal closure.

If a covariate effect was significant, then the associated antecedent importance weights ω_j reveal the temporal response pattern to the environmental variable. A significant time lag exists between plant Ψ and X_j if, first, the 95% CI of a particular ω_j does not overlap the prior mean (a flat prior gives a prior mean of $1/T_{lag}$) or if, second, the 95% CI of one or more ω_j does not contain the posterior mean of an ω_j for another past time period. For ω_j values with narrow CIs, the posterior means indicate the relative contribution of that variable at the corresponding time step to the overall antecedent variable; wide CIs signify potential difficulty in resolving the timescales of influence.

The Bayesian models (Eqns (1)–(4b) and corresponding priors) were implemented in JAGS 4.2.0 (Plummer, 2003) via R (R Core Team, 2016), using the packages 'RJAGS' (Plummer, 2013) and 'CODA' (Plummer *et al.*, 2006). Three parallel Markov chain Monte Carlo (MCMC) sequences were assigned widely dispersed starting values, and initial iterations were run until convergence was achieved as measured by the Gelman statistic (Gelman & Rubin, 1992). Raftery and Lewis's diagnostic (Raftery & Lewis, 1992) was performed on initial chains to determine required MCMC sample size. These diagnostics led us to run 200 000 (400 000) iterations for the Ψ_B (Ψ_D) model, and to thin the sequences by 40 (80) to obtain a posterior sample size of 5000 for each parameter. Thinning was implemented to reduce both within-chain autocorrelation and storage requirements.

Results

Model fit

A regression of predicted vs observed plant Ψ yielded $R^2 = 0.84$ for Ψ_B and 0.65 for Ψ_D (Table 2; Fig. S2), which represented improved model fit by ~0.1 from models without antecedent covariates (Methods S2, $R^2 = 0.74$ and 0.56 respectively). Both models showed some bias (slopes of predicted vs observed of 0.80 and 0.61 respectively), with underestimation at high (less negative) Ψ and overestimation at low (more negative) Ψ, particularly for Ψ_D (Fig. S2b). Such bias is typical of hierarchical models that allow for borrowing of strength (e.g. among shrub-level parameters; Greenland, 2000), but greater borrowing of strength reduces the effective numbers of parameters (here, $\Psi_B = 44.1$ and $\Psi_D = 105.3$; Spiegelhalter *et al.*, 2002). When predicted and observed plant Ψ were averaged across individual shrubs (for each round of measurements) to yield estimates of mean plant Ψ for all shrubs, model fit ($R^2 = 0.94$ for Ψ_B and 0.76 for Ψ_D) and bias (slope: 0.89 for Ψ_B and 0.68 for Ψ_D) improved for both models (Fig. S3).

Covariate effects

Variation in Ψ_B was primarily explained by the main effects of the daily-scale antecedent variables: maximum vapor pressure deficit max D^{ant}, shallow soil water W_{30}^{ant}, and deep soil water W_{60}^{ant}; none of their interaction terms were significant (see Table 3 for coefficient estimates, Fig. 2a). Both max D^{ant} and W_{60}^{ant} exerted negative effects on Ψ_B, whereas W_{30}^{ant} exerted a positive influence. The covariate effects (posterior means and 95% CIs) associated with the Ψ_B model were fairly similar across shrubs and treatments, although three and seven out of 16 shrubs did not experience the negative effects of max D^{ant} and W_{60}^{ant} respectively. Population-level Ψ_B at nominal environmental conditions (intercept, μ_{β_0}) was estimated at −3.4 MPa (posterior mean), with minimal variation among shrubs or treatments and relatively narrow CIs (Fig. S4).

Variation in Ψ_D was associated with the same significant main effects as for Ψ_B: the effects of max D^{ant}, W_{30}^{ant} and W_{60}^{ant} had the same direction and similar magnitudes across both models (Table 3; Fig. 2b). However, the covariate effects associated with the Ψ_D model exhibited greater variability among shrubs and treatments than the Ψ_B model did. Although shrubs in both treatment groups experienced a similar positive effect of W_{30}^{ant} on Ψ_D, control and watered shrubs were differentially affected by max D^{ant} and W_{60}^{ant}. Ψ_D of control shrubs was negatively affected by max D^{ant} and not by W_{60}^{ant}, whereas Ψ_D of watered shrubs was negatively affected by W_{60}^{ant} and not by max D^{ant}. Moreover, unlike the Ψ_B model, several interaction terms were significant in the Ψ_D model, at both the population and treatment levels (Table 3; Fig. 2b,c). The max $D^{ant} \times W_{30}^{ant}$ and max $D^{ant} \times W_{60}^{ant}$ terms were significantly negative, indicating that high (low) soil moisture at either depth enhances (reduces) the negative effect of max D^{ant} on Ψ_D (Fig. S5a, b). The population-level Ψ_D at nominal environmental conditions μ_{α_0} was estimated to be −3.8 MPa (Fig. S4), and shrub-level means did not differ significantly among treatment groups. However, control shrubs had greater between-shrub variation in posterior means and wider CIs than watered shrubs.

Since Ψ_D varies on a subdaily timescale, we also evaluated responses to antecedent half-hourly D variables (D^{ant} and ΔD^{ant}), which were not considered in the daily-scale Ψ_B model. Surprisingly, the main effects of D^{ant} and ΔD^{ant} were not significant (Fig. 2c); however, these variables often interacted significantly with daily-scale antecedent covariates to affect Ψ_D. For example, the effect of W_{30}^{ant} was modified by half-hourly D variables such that high D^{ant} reduced the positive effect of W_{30}^{ant} on Ψ_D (Fig. S5c). Moreover, the significant $W_{30}^{ant} \times \Delta D^{ant}$ interaction indicates a hysteretic pattern, wherein the positive effect of W_{30}^{ant} on Ψ_D is stronger when D is increasing ($\Delta D^{ant} > 0$) than when D is decreasing (Fig. S5d, $\Delta D^{ant} < 0$). The positive max$D^{ant} \times D^{ant}$ interaction indicates that Ψ_D is negatively correlated with D^{ant} only when maxD^{ant} is low (Fig. S5e). Finally, the $D^{ant} \times \Delta D^{ant}$

Table 2 Population-, treatment- and shrub-level summary of baseline water potential Ψ_B and diurnal water potential Ψ_D model fit results, including the intercept, slope, coefficient of determination R^2, and sample size n associated with regressions of predicted vs observed plant Ψ values (see Supporting Information Fig. S2 for population-level results)

Level	Ψ_B Intercept	Slope	R^2	n	Ψ_D Intercept	Slope	R^2	n
Population	−0.603	0.794	0.838	151	−1.326	0.615	0.653	885
Control	−0.688	0.753	0.811	75	−1.536	0.559	0.596	442
Shrub 1	−0.069	0.997	0.979	5	−0.808	0.748	0.818	13
Shrub 2	−0.144	0.875	0.970	5	−0.535	0.816	0.864	12
Shrub 3	−0.234	0.890	0.932	4	−0.479	0.844	0.938	12
Shrub 4	−0.518	0.838	0.899	5	−0.414	0.871	0.909	13
Shrub 5	−0.656	0.781	0.889	14	−1.658	0.555	0.623	103
Shrub 6	−1.023	0.666	0.693	14	−1.577	0.564	0.569	94
Shrub 7	−1.239	0.571	0.530	14	−1.616	0.530	0.542	93
Shrub 8	−1.287	0.490	0.466	14	−2.325	0.281	0.276	102
Watered	−0.522	0.834	0.863	76	−1.109	0.674	0.713	443
Shrub 9	0.020	1.017	0.994	4	−0.570	0.841	0.922	12
Shrub 10	0.598	1.338	0.977	5	−0.399	0.894	0.862	15
Shrub 11	−0.270	0.905	0.945	6	−0.552	0.848	0.916	13
Shrub 12	−0.480	0.816	0.937	14	−1.047	0.690	0.736	94
Shrub 13	−0.446	0.888	0.920	5	−0.619	0.835	0.955	12
Shrub 14	−0.806	0.734	0.812	14	−1.339	0.596	0.645	102
Shrub 15	−0.796	0.744	0.734	14	−1.226	0.628	0.637	101
Shrub 16	−0.843	0.717	0.687	14	−1.314	0.622	0.629	94

Shrubs 1–8 belong to the control group; shrubs 9–16 received supplemental irrigation (watered). Shrubs are ordered by descending R^2 for the Ψ_B model. Population refers to the overall population of 16 shrubs.

Table 3 Population-level regression coefficients for the baseline water potential Ψ_B and diurnal water potential Ψ_D models, their associated covariate, posterior mean (mean), and 95% central credible interval (95% CI)

Coef.	Associated covariate	Mean	95% CI
Baseline (Ψ_B) model			
μ_{β_0}	Intercept	**−3.398**	(−3.631, −3.191)
μ_{β_1}	max D^{ant}	**−0.334**	(−0.489, −0.185)
μ_{β_2}	W_{30}^{ant}	**0.186**	(0.137, 0.232)
μ_{β_3}	W_{60}^{ant}	**−0.222**	(−0.391, −0.080)
$\mu_{\beta_{1,2}}$	max $D^{ant} \times W_{30}^{ant}$	−0.005	(−0.042, 0.028)
$\mu_{\beta_{1,3}}$	max $D^{ant} \times W_{60}^{ant}$	−0.044	(−0.157, 0.062)
$\mu_{\beta_{2,3}}$	$W_{30}^{ant} \times W_{60}^{ant}$	0.007	(−0.018, 0.028)
Diurnal (Ψ_D) model			
μ_{α_0}	Intercept	**−3.811**	(−4.169, −3.423)
μ_{α_1}	max D^{ant}	**−0.262**	(−0.508, −0.068)
μ_{α_2}	W_{30}^{ant}	**0.171**	(0.104, 0.220)
μ_{α_3}	W_{60}^{ant}	**−0.329**	(−0.531, −0.150)
μ_{α_4}	D^{ant}	−0.023	(−0.101, 0.047)
μ_{α_5}	ΔD^{ant}	−0.183	(−0.559, 0.222)
$\mu_{\alpha_{1,2}}$	max $D^{ant} \times W_{30}^{ant}$	**−0.037**	(−0.081, −0.007)
$\mu_{\alpha_{1,3}}$	max $D^{ant} \times W_{60}^{ant}$	**−0.125**	(−0.231, −0.023)
$\mu_{\alpha_{1,4}}$	max $D^{ant} \times D^{ant}$	**0.030**	(0.008, 0.053)
$\mu_{\alpha_{1,5}}$	max $D^{ant} \times \Delta D^{ant}$	0.149	(−0.279, 0.450)
$\mu_{\alpha_{2,3}}$	$W_{30}^{ant} \times W_{60}^{ant}$	0.009	(−0.017, 0.042)
$\mu_{\alpha_{2,4}}$	$W_{30}^{ant} \times D^{ant}$	**−0.017**	(−0.029, −0.004)
$\mu_{\alpha_{2,5}}$	$W_{30}^{ant} \times \Delta D^{ant}$	**0.163**	(0.080, 0.236)
$\mu_{\alpha_{3,4}}$	$W_{60}^{ant} \times D^{ant}$	0.016	(−0.056, 0.060)
$\mu_{\alpha_{3,5}}$	$W_{60}^{ant} \times \Delta D^{ant}$	−0.042	(−0.256, 0.201)
$\mu_{\alpha_{4,5}}$	$D^{ant} \times \Delta D^{ant}$	**−0.411**	(−0.680, −0.112)

Significant coefficients are in bold, as indicated by 95% CIs that do not contain zero. See Table 1 for definitions of the covariates; see Fig. 2 and Supporting Information Fig. S4 for shrub-level estimates.

interaction was significantly negative, leading to another case of hysteresis: Ψ_D decreases with D when D is increasing ($\Delta D^{ant} > 0$), yet Ψ_D increases with D when D is decreasing ($\Delta D^{ant} < 0$) (Fig. S5f).

Though the main effect of D^{ant} was not significant, some combinations of antecedent daily soil and atmospheric moisture conditions yield significantly positive or negative sensitivities ($S_{\Psi,D} = d\Psi_D/dD^{ant}$), depending on the sign of ΔD^{ant}. Negative $S_{\Psi,D}$ (increasing D^{ant} leads to more negative Ψ_D, and vice versa) dominates when ΔD^{ant} is positive (morning), and the magnitude increases under more favorable (wetter) antecedent moisture conditions (Fig. 3a). By contrast, positive $S_{\Psi,D}$ (increasing D^{ant} leads to less negative Ψ_D, and vice versa) occurs when ΔD^{ant} is negative (afternoon), with increasing magnitude under less favorable (drier) antecedent moisture conditions (Fig. 3c). Neutral values of $S_{\Psi,D}$ (Ψ_D not responsive to D^{ant}) can occur across a range of antecedent moisture conditions, but primarily when antecedent conditions are dry and ΔD^{ant} is positive (Fig. 3a) or when antecedent conditions are wet and ΔD^{ant} is negative (Fig. 3c). When $\Delta D^{ant} \approx 0$ (midday), $S_{\Psi,D}$ spans negative, neutral, or positive values, depending on antecedent moisture conditions (Fig. 3b).

Antecedent weights

While the covariate effects were modeled hierarchically, antecedent weights ω were only modeled at the population level. For Ψ_B, ω for max D^{ant} peaked 4 d before the Ψ_B measurement (Fig. 4a). The ω for W_{30}^{ant} and W_{60}^{ant} were associated with different timescales of influence: the highest ω for W_{30}^{ant} occurred on the day leading up to the Ψ_B measurement (Fig. 4b), indicating

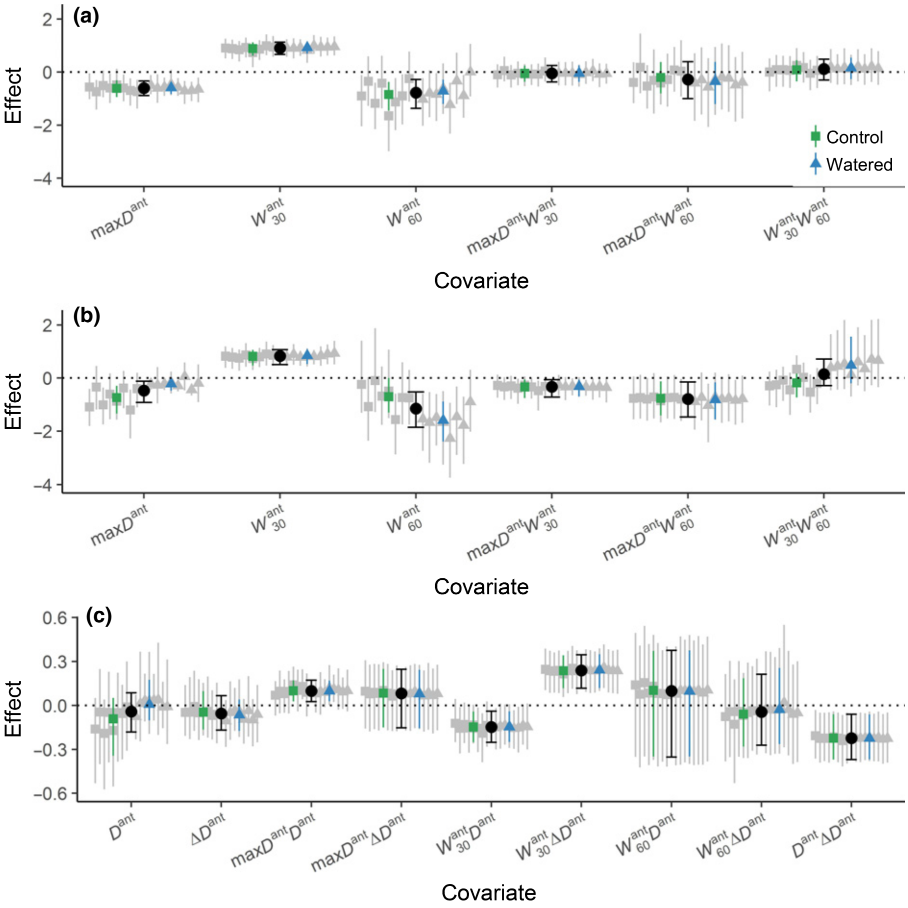

Fig. 2 Posterior means and 95% central credible intervals (CIs) for the population-level (black), treatment-level (colored), and shrub-level (gray) regression parameters (coefficients) for each covariate in the (a) baseline water potential Ψ_B model and the (b, c) diurnal water potential Ψ_D model. (a, b) The analogous regression parameters from the Ψ_B and Ψ_D models respectively, and (c) shows the remaining Ψ_D regression parameters related to half-hourly covariates. Regression coefficients are normalized by dividing their posterior means and CI limits by the empirical standard deviations of each covariate. See Table 1 for definitions of covariates; see Supporting Information Fig. S4 for the corresponding intercept estimates.

that current shallow moisture has the strongest influence on Ψ_B, with no lag period. By contrast, the highest ω for W^{ant}_{60} occurred 6–7 d before the Ψ_B measurement (Fig. 4c), reflecting a week-long time lag and a much longer timescale of influence.

With respect to the Ψ_D response, which included the effects of daily and subdaily scale covariates, the ω for max D^{ant} was highest 2 d before the Ψ_D measurement (Fig. 4d). Interestingly, the ω for W^{ant}_{30} was similarly high for 1 and 7 d prior (Fig. 4e), a bimodal pattern that indicates an effect of W^{ant}_{30} on multiple timescales. For W^{ant}_{60}, ω was extremely low for 1 to 5 d into the past, moderate for 6 d ago, and highest for 7 d ago (Fig. 4f), mirroring the temporal pattern of the W^{ant}_{60} weights in the Ψ_B model. With respect to the diurnal (half-hourly) variables affecting Ψ_D, ω for D^{ant} was highest for the concurrent half-hour and quickly attenuated thereafter (Fig. 5a), whereas ΔD^{ant} had the highest ω for the concurrent half-hour and 3 h ago (Fig. 5b), indicating another potential bimodal timescale response.

Discussion

Upon applying the SAM framework to repeated measurements of Ψ_B and Ψ_D and associated atmospheric and soil moisture indices *D* and *W*, we broadly found that while *Larrea* Ψ_B is governed by the main effects of daily-scale *D* and *W*, Ψ_D is interactively controlled by *D* and *W* at multiple timescales. Furthermore, the response of Ψ_D to subdaily *D* depends upon past conditions, indicating diurnal hysteresis. However, owing to sampling of plant Ψ primarily during the summer growing season (Fig. S1), our results may reflect this particular study period rather than broader patterns of *Larrea* Ψ. in the following we discuss Q1 and Q2 (the effect and temporal scales of environmental drivers of Ψ) first for atmospheric moisture, then for soil moisture. We subsequently address Q3 and interpret the interactive influence of antecedent conditions on the regulation of Ψ_D.

Atmospheric moisture controls plant Ψ on multiple timescales

Higher vapor pressure deficit *D* increases the driving gradient for transpiration, which increases tension on the water column and is expected to result in more negative plant Ψ (Sperry *et al.*, 2002). Though this expectation generally applies to subdaily variation in Ψ_D (Jarvis, 1976), our analyses indicate an analogous lagged effect of past *D*. Antecedent maximum daily D (max D^{ant},

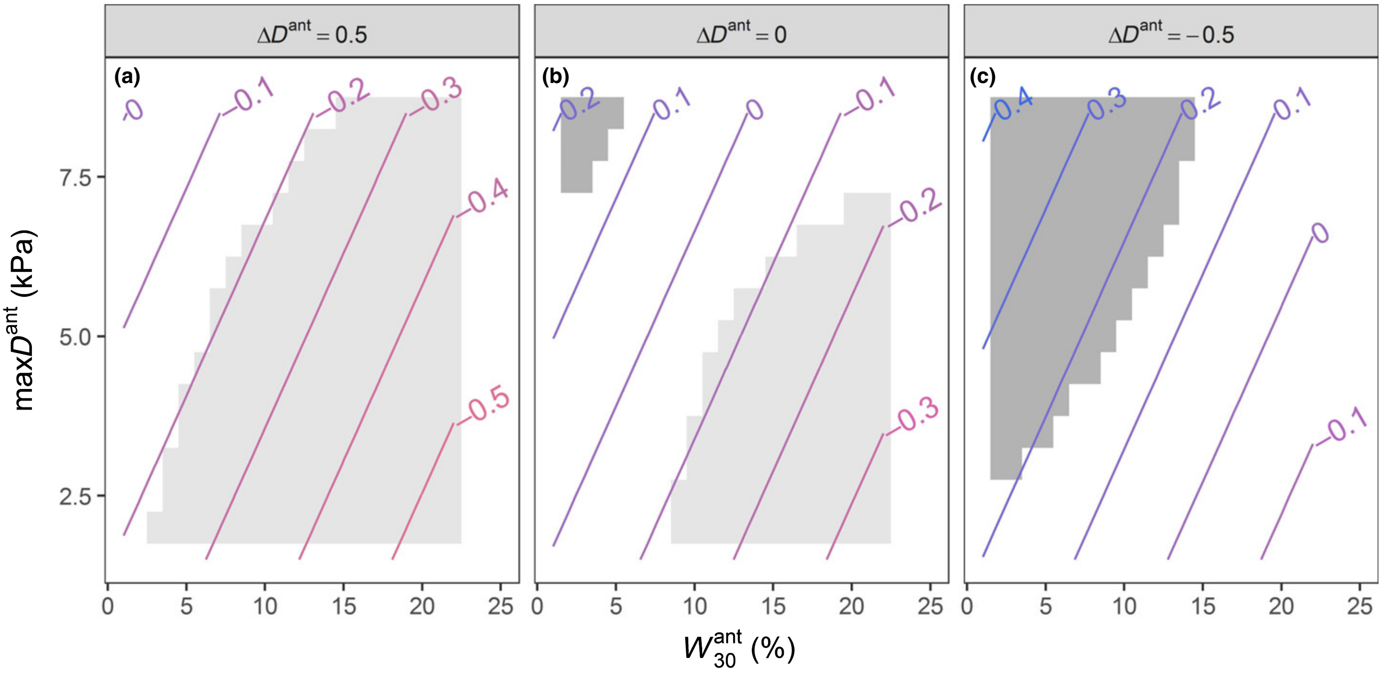

Fig. 3 Estimated sensitivities ($S_{\Psi,D} = d\Psi_D/dD^{ant}$) of diurnal water potential Ψ_D to changes in antecedent half-hourly vapor pressure deficit D^{ant} for a range of antecedent shallow soil water (W_{30}^{ant}) and antecedent daily maximum D ($\max D^{ant}$) values at three levels of antecedent half-hourly changes in D: (a) $\Delta D^{ant} = 0.5$ kPa ('morning'), (b) $\Delta D^{ant} = 0$ kPa ('midday'), and (c) $\Delta D^{ant} = -0.5$ kPa ('afternoon'). $S_{\Psi,D}$ was calculated within the Bayesian Markov chain Monte Carlo simulations to propagate uncertainties in the parameters (i.e. relevant α values). The contours represent the posterior means for $S_{\Psi,D}$ (MPa/kPa); the lighter shaded regions indicate significant negative sensitivities ($S_{\Psi,D} < 0$), whereas the darker shaded regions represent significant positive sensitivities ($S_{\Psi,D} > 0$). The unshaded regions represents neutral sensitivities ($S_{\Psi,D}$ not significantly different from zero).

hereafter 'daily D') negatively affected both Ψ_B and Ψ_D, indicating that prior exposure to dry (moist) atmospheric conditions resulted in more (less) negative plant Ψ. *Larrea* appears to retain the negative impact of past atmospheric drought for multiple days. Specifically, Ψ_B and Ψ_D exhibited lags of 4 d and 2 d respectively in response to variation in daily D, which could possibly reflect hormonal transport times, xylem embolism, or depletion of surface soil moisture. Foliar-derived abscisic acid (ABA) can be transported basally via phloem (Ikegami *et al.*, 2009; Manzi *et al.*, 2015; McAdam *et al.*, 2016) and may impact root growth (McAdam *et al.*, 2016), stomatal conductance (Mitchell *et al.*, 2017), and potentially plant Ψ. The observed multi-day lag between daily-scale maximum D and plant Ψ may be due to the relatively slow transport time of foliar ABA to roots (Mencuccini & Hölttä, 2010). Cumulative high-D events could also cause progressive cavitation fatigue (Hacke *et al.*, 2001), which could manifest as a lagged effect of D on plant Ψ. Finally, past D could influence plant Ψ through evaporation of surface soil moisture. Although the model directly accounts for the integrated effects of soil moisture from 0 to 30 cm and 30 to 60 cm, a small but significant amount of *Larrea*'s active roots are found in the top 2 cm of the soil (Ogle *et al.*, 2004), where soil moisture is strongly affected by evaporation (Kidron, 2009). Previously high D could exacerbate evaporation from the surface soil, resulting in apparent lagged declines in plant Ψ in response to daily D.

Whereas Ψ_B responded independently to atmospheric and soil moisture stress, Ψ_D responses to daily D were modulated by antecedent soil moisture. The negative effect of daily D is enhanced when either shallow or deep W is (or has been) high, another potential indication of hormone signaling effects. For example, dry soil can trigger an ABA signal that results in stomatal closure (Wilkinson & Davies, 2002), but wet soil may prevent such hormone signaling, thus reducing stomatal sensitivity to D (Tardieu & Davies, 1992). Contrasting signals from wet soil and a dry atmosphere may permit *Larrea*'s Ψ to decline, as stomata remain open to ensure carbon acquisition under moist soil conditions.

Though we expected a negative relationship between Ψ_D and half-hourly D (D^{ant}, hereafter 'subdaily D'), the significance and direction of the effect depended upon antecedent daily-scale moisture variables ($\max D^{ant}$ and W_{30}^{ant}) as well as the directional change in D (as captured by ΔD^{ant}). Under relatively moist antecedent soil and atmospheric conditions, Ψ_D exhibits the expected negative relationship with subdaily D in the morning ($\Delta D^{ant} > 0$) and a neutral relationship in the afternoon ($\Delta D^{ant} < 0$), even when past daily D is high (Fig. 3a,c). This pattern in Ψ_D aligns with *Larrea*'s natural circadian pattern of photosynthesis, wherein photosynthesis peaks in the morning hours (Bamberg *et al.*, 1975) followed by frequent midday and afternoon depressions (Naumburg *et al.*, 2003). By contrast, under *dry* antecedent moisture conditions, subdaily D has no impact on Ψ_D in the morning (Fig. 3a), and higher values in the afternoon (Fig. 3c) correspond to less negative Ψ_D. It is not uncommon for maximum Ψ_D in *Larrea* to become less negative than Ψ_B in dry soils (Syvertsen *et al.*, 1975), as occurred on two of our sampling dates (Fig. 1) following 19 consecutive dry days. Such dry

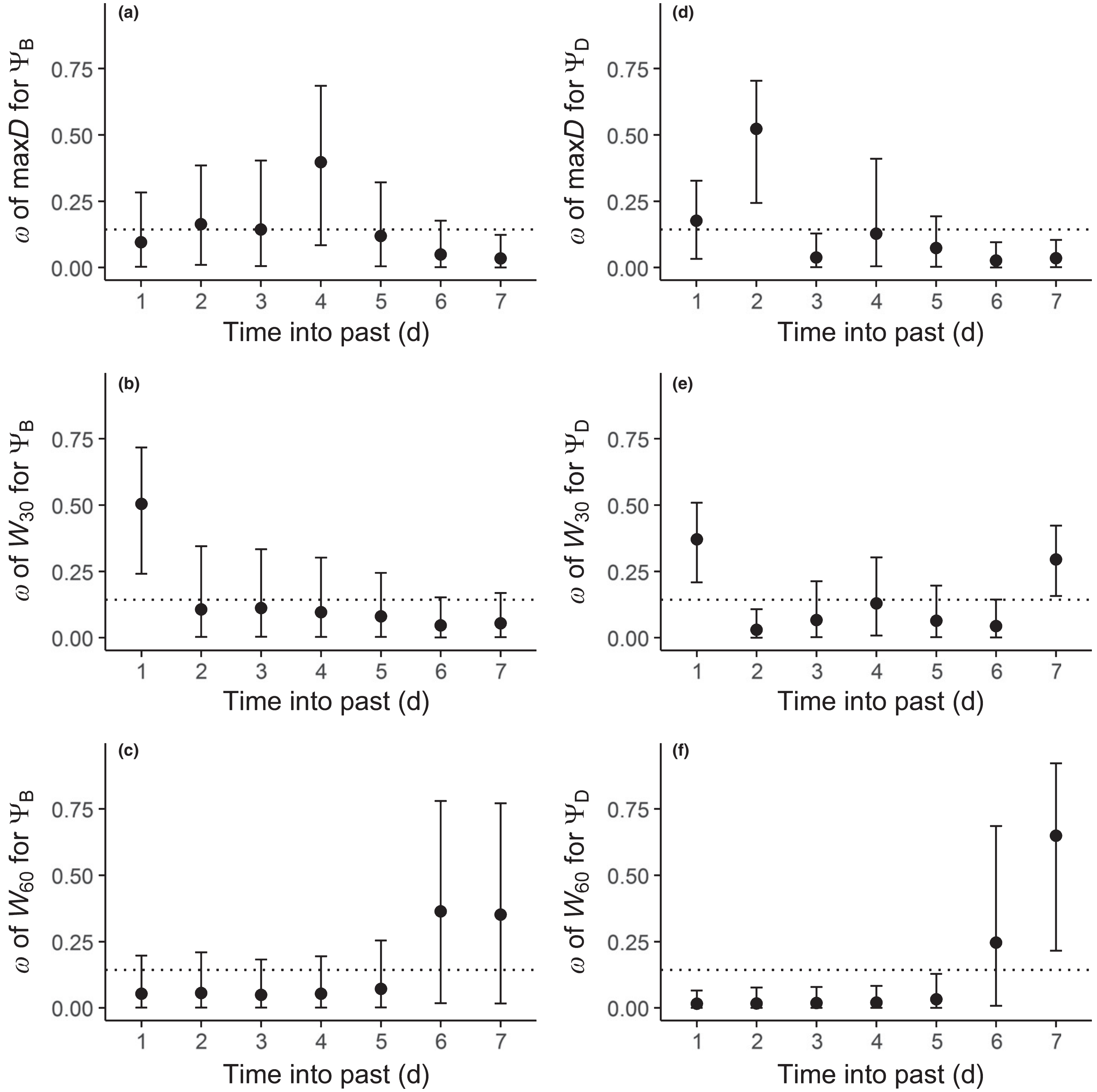

Fig. 4 Posterior means and 95% central credible intervals for antecedent weights ω associated with (a, d) daily max D, (b, e) daily W_{30}, and (c, f) daily W_{60}. (a–c) From the baseline water potential Ψ_B model; (d–f) from the diurnal water potential Ψ_D model. The dotted horizontal line represents the prior mean. See Table 1 for definitions of covariates.

antecedent conditions may prompt ABA production in the guard cells of the stomata (Virlouvet & Fromm, 2015), triggering low rates of morning photosynthesis and stomatal closure in the afternoon, which would allow Ψ_D to recover to less negative values (Tenhunen *et al.*, 1982). The variable sensitivity of Ψ_D to subdaily D highlights how acclimation to antecedent conditions can modify the underlying circadian pattern of stomatal behavior and Ψ_D (Lange *et al.*, 1982; Hennessey & Field, 1991; Mencuccini *et al.*, 2000).

Because circadian controls also affect diurnal carbon and water fluxes in plants (Doughty *et al.*, 2006; Resco de Dios *et al.*, 2016), diurnal hysteresis has often been observed between indices of plant water use and environmental drivers (Jarvis, 1976; O'Grady *et al.*, 1999; Zhang *et al.*, 2014). Hysteresis in Ψ_D was detected in our analysis via significant interactions between the covariate ΔD^{ant} (an index of time of day) and both shallow soil moisture W_{30} and subdaily D. W_{30} had a stronger positive effect on Ψ_D when D was increasing ($\Delta D^{\mathrm{ant}} > 0$) than when D was

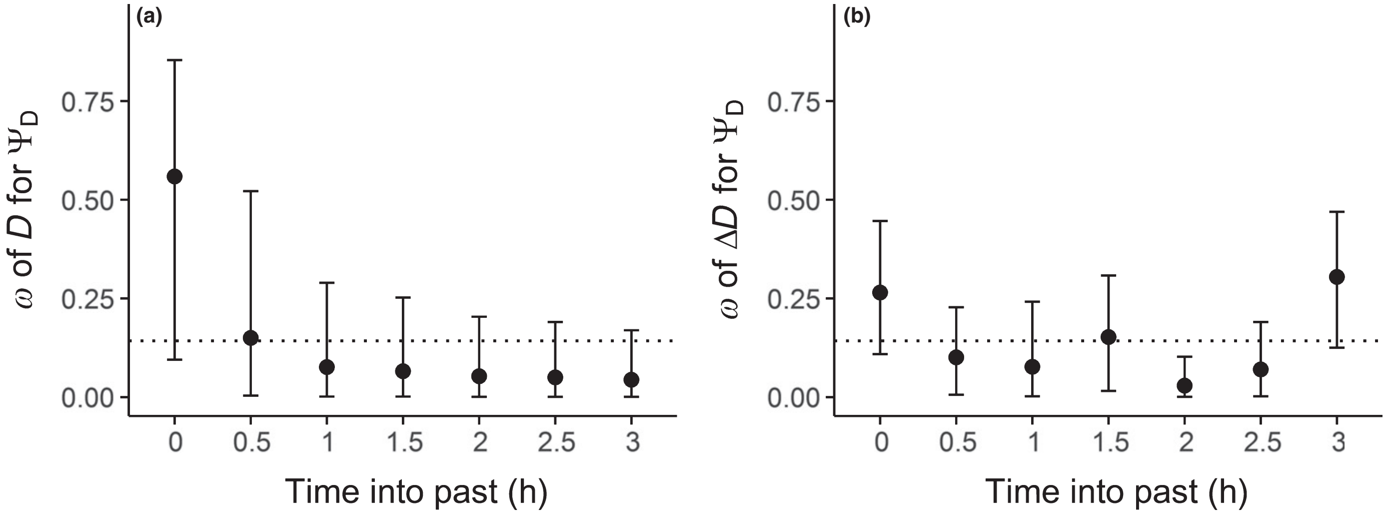

Fig. 5 Posterior means and 95% central credible intervals for antecedent weights ω associated with (a) subdaily D and (b) subdaily ΔD from the diurnal water potential Ψ_D model. The dotted horizontal line represents the prior mean. See Table 1 for definitions of covariates.

decreasing ($\Delta D^{ant} < 0$). This suggests that the effect of past soil moisture varies throughout *Larrea*'s diurnal course of plant Ψ; past soil moisture has a strong effect in the morning, when transpiration, conductance, and photosynthesis are generally the highest, but less impact on Ψ_D in the afternoon, during midday stomatal closure. Such hysteresis in Ψ_D matches hysteretic responses of stomata to D in a *Populus* hybrid (Meinzer *et al.*, 1997), wherein transpiration rates at the same D are higher in the morning vs the afternoon of the same day. Causes of hysteresis in response to changing D are not well understood, but may be driven by the contribution of stored water in the stem, changes in soil-to-leaf hydraulic conductivity (O'Grady *et al.*, 1999), or determined by underlying circadian rhythms (Hennessey & Field, 1991; Resco de Dios *et al.*, 2016).

In general, subdaily D (D^{ant} and ΔD^{ant}) affects Ψ_D through interactions with antecedent daily-scale D and shallow W, suggesting that Ψ_D responses integrate over multiple timescales. Ψ_D responds to subdaily D in near real time (no lag), such that the conditions occurring in the half-hour concurrent to observed Ψ_D were the most important. Stomatal conductance of these same shrubs also exhibited a short lag with respect to subdaily D (Ogle *et al.*, 2015), indicating that fast Ψ_D responses are likely driven by stomata that are tightly coupled to variable atmospheric conditions (Damour *et al.*, 2010). Because the effect of subdaily D interacts significantly with daily-scale moisture variables, Ψ_D responds to environmental conditions over multiple timescales, from hours to days. This suggests that *Larrea* can acclimate to dry antecedent conditions over multiple days and respond by decreasing Ψ sensitivity to subdaily D, likely through stomatal acclimation to past atmospheric (Kutsch *et al.*, 2001) and soil moisture conditions (Ludlow *et al.*, 1985).

Soil moisture effects on plant Ψ depend on depth and cumulative moisture status

Interestingly, shallow and deep W had opposite effects on plant Ψ (Ψ_B and Ψ_D). In both treatments groups (control vs watered), as expected, wetter shallow W is associated with increased (less negative) plant Ψ, because additional soil moisture increases the supply of water to the roots and transpiration stream. In many deserts, most rain events primarily recharge surface soil layers, leading to notable temporal variation in shallow W, while deep W can remain fairly constant over time (Scanlon, 1994), leading to temporal decoupling between shallow and deep soil moisture (e.g. Fig. S1c–f). In general, *Larrea* root biomass is confined to shallow or intermediate depths (e.g. 10–30 cm; Montaña *et al.*, 1995; Briones *et al.*, 1996), and roots in the subsurface (e.g. 0–10 cm) are capable of water uptake following rains (Ogle *et al.*, 2004), which accounts for the positive relationship between plant Ψ and shallow W. By contrast, we generally found a negative relationship between plant Ψ and deep W (Fig. 2a,b). Roots at intermediate or deeper depths (20–45 cm) are primarily responsible for water uptake in *Larrea* at this site (Ogle *et al.*, 2004), and some large shrubs can access relatively stable deeper soil moisture (Franco *et al.*, 1994). Therefore, a reliable supply of deep (30–60 cm) soil water may permit stomata to avoid closure and become less sensitive to D (Hinckley *et al.*, 1983), resulting in more negative Ψ_B and Ψ_D as the plant continues to photosynthesize and transpire in response to 'available' deep soil water. Overall, *Larrea* appears to regulate plant Ψ by responding differently to shallow vs deep soil moisture.

In general, plant Ψ_B and Ψ_D responded to concurrent shallow W but exhibited a lagged (6–7 d) response to deep W, which mirrors the timescales of influence uncovered for stomatal conductance in *Larrea* (Ogle *et al.*, 2015). However, Ψ_D displayed a bimodal lagged response to shallow W, which was strongly influential both 1 and 7 d before measurement. Differential lags for shallow vs deep W could be a function of *Larrea*'s bimodal rooting distribution (Ogle *et al.*, 2004), as well as the dynamics of root conductivity, growth, and mycorrhizal associations. The 1-d lagged responses of both Ψ_B and Ψ_D to shallow W may result from water uptake by existing shallow roots that maintain high conductivity (Hultine *et al.*, 2006). For example, the C_4 grass *Bouteloua gracilis* increased plant Ψ within 1 d of a simulated

5 mm rain event (Sala & Lauenroth, 1982) as the result of water uptake by existing, functional roots (Lauenroth *et al.*, 1987). The 6- and 7-d lagged responses of plant Ψ_B and Ψ_D to deep W could be driven by both recovery of hydraulic conductivity and new growth belowground. In the desert succulent *Agave deserti*, partial recovery of root hydraulic conductivity was achieved after 7 d of rewetting, with full recovery attributed to new root growth (North & Nobel, 1995). New root growth can further aid the absorption of water by increasing root contact with wet soil (Caldwell, 1976), but may lag behind the initial recharge of soil moisture due to high soil temperatures or *Larrea*'s high oxygen requirements for root growth (Lunt *et al.*, 1973). Finally, colonization by arbuscular mycorrhizal fungi following rainfall (Titus *et al.*, 2002) may enhance *Larrea*'s water status, though slow colonization rates (Apple *et al.*, 2005) could also contribute to the 6–7 d lag responses. Soil moisture in deep layers is also less impacted by evapotranspiration and may have a longer residence time (Sala *et al.*, 1992; Ng *et al.*, 2015), resulting in a longer lag effect of deep W on plant Ψ.

Different primary drivers of Ψ_D were significant for control and watered shrubs, suggesting prolonged legacy effects of soil moisture availability. Though Ψ_D of both treatment groups increased with wetter shallow W, control and watered shrubs had differential Ψ_D responses to daily-scale atmospheric and deep soil moisture (Fig. 2b). Antecedent daily D regulated Ψ_D of control shrubs, whereas Ψ_D of watered shrubs was negatively affected by deep W, suggesting that large moisture pulses that infiltrate deeper soil layers can fundamentally alter regulation of plant Ψ. In desert ecosystems, plant physiological responses may only be triggered by 'biologically important' amounts of precipitation (Beatley, 1974; Fernández, 2007). Though irrigation was only applied three times during the study period, the magnitudes of the applications exceeded most single precipitation events that occurred during the study period (Fig. S1). The surplus water inputs could push watered shrubs past a threshold W that suppressed the response of watered shrubs' Ψ_D to antecedent daily D. Because antecedent daily D was not a significant driver of Ψ_D in watered shrubs, watered shrubs appeared to have weaker 'memory' of past D extremes. The increased deep W may provide a long-term water source for transpiration such that the plant can routinely avoid stomatal closure, rendering Ψ_D insensitive to antecedent daily D. Therefore, large irrigation (or rain) events that affect both shallow and deep W can apparently exert a long-term (months–seasons) legacy effect on plant Ψ that is not captured by antecedent daily-scale variables.

The relationship between Ψ_B, Ψ_D, and environmental drivers (D and W) are well understood and can be modeled mechanistically (e.g. Sperry *et al.*, 2016). However, it remains to be seen whether mechanistic models can capture the effect of antecedent conditions through simulation of the biophysical process. Future work could address whether lagged responses emerge from plant hydraulic models that explicitly include mechanisms linking stomatal behavior, plant Ψ, soil moisture, and vapor pressure deficit. If lagged responses are not captured through the biophysics of water transport, then additional representation of physiology (e.g. ABA transport, acclimation) may be needed.

Dynamic shifts in water potential regulation

The Ψ_D was positively, negatively, or not significantly correlated with subdaily D depending on time of day and antecedent moisture conditions, suggesting dynamic stomatal regulation of plant Ψ in *Larrea*. Negative sensitivity to D ($S_{\Psi,D} < 0$) in the mornings ($\Delta D^{ant} > 0$) suggests weak stomatal regulation such that Ψ_D becomes more negative as D increases. Neutral sensitivity ($S_{\Psi,D} \approx 0$) can occur at any time of day and implies strong stomatal regulation such that Ψ_D does not change in response to changing D. Finally, positive sensitivity to D ($S_{\Psi,D} > 0$) in the afternoons ($\Delta D^{ant} < 0$) suggests excessive stomatal closure such that Ψ_D becomes less negative under higher D, which we deem as overcompensating behavior. Importantly, our results suggest that weak stomatal regulation and overcompensation are unlikely to occur within the same day. For example, the highlighted (light and dark gray) areas of significant negative and positive $S_{\Psi,D}$ barely overlap for the same daily-scale antecedent variables (Fig. 3). Under moist antecedent conditions, $S_{\Psi,D}$ can shift from negative to neutral during a single day. However, under dry antecedent conditions, $S_{\Psi,D}$ can shift from neutral to positive within a day. Such overcompensating stomatal behavior during dry antecedent conditions may explain how Ψ_D can recover to, and sometimes even exceed, Ψ_B (Syvertsen *et al.*, 1975; Fig. 1). While concurrent environmental conditions are known to influence midday stomatal closure and recovery of Ψ_D (Schulze *et al.*, 1974; Tenhunen *et al.*, 1982), we demonstrate the importance of antecedent moisture status in regulating Ψ_D patterns. Given that Ψ_D lags daily-scale D (max D) by 2–4 d and lags W_{30} by 1 and 7 d, shifts in plant Ψ regulation may occur in under 1 wk, which may be advantageous in a mostly dry ecosystem with pulsed moisture inputs (Noy-Meir, 1973; Loik *et al.*, 2004). *Larrea*'s Ψ and stomatal conductance (Ogle *et al.*, 2015) have similar temporal responses to soil and atmospheric moisture conditions, confirming that regulation of plant Ψ is strongly coordinated by stomatal behavior.

We propose that *Larrea* is able to adjust regulation of plant Ψ as a result of past soil and atmospheric moisture conditions. Furthermore, our analysis revealed an unexpected positive sensitivity of plant Ψ to D ($S_{\Psi,D} > 0$) indicative of overcompensating stomatal regulation; this syndrome could be common to desert shrubs that experience midday stomatal closure and Ψ recovery under high D (Tenhunen *et al.*, 1982; Nilsen *et al.*, 1983). *Larrea*'s ability to dynamically shift between weak, strong, and overcompensating regulation of plant Ψ depending on past moisture conditions could be key to its dominance in the hot deserts of North America (Smith *et al.*, 1997). More generally, we suggest that subdaily measurements of plant Ψ will be invaluable for expanding current conceptions of iso-/anisohydry spectrum (Klein, 2014; Martínez-Vilalta *et al.*, 2014; Hochberg *et al.*, 2018) to encompass overcompensating stomatal regulation and condition-dependent plant Ψ sensitivity to D.

Conclusion

Our results suggest that *Larrea*'s baseline and diurnal plant Ψ are interactively controlled by atmospheric and soil moisture conditions (D and W respectively) at multiple timescales and well coordinated with temporal patterns of stomatal conductance (Ogle *et al.*, 2015). This is not surprising given the history of research that indicates that plant water status and stomatal behavior are controlled by D and W (Dixon & Joly, 1895; Jarvis, 1976; Sperry *et al.*, 2002). However, we refined the classic understanding of plant Ψ by quantifying the temporal lags of associated atmospheric and soil moisture drivers at two temporal scales: daily and subdaily. We found evidence of a hysteretic effect of subdaily D on diurnal plant Ψ, highlighting the importance of circadian rhythms. The variation in sensitivity of Ψ to subdaily D depends upon antecedent daily-scale D and W conditions, likely reflecting rapid shifts in plant Ψ regulation. We identified a positive sensitivity of *Larrea*'s Ψ to D, indicating possible overcompensating stomatal regulation of plant Ψ. Changes in plant Ψ sensitivity to D are also evident in the 2–4 d lagged response of baseline and diurnal plant Ψ to maximum daily D. Moreover, the timescales of influence associated with soil moisture depended on the depth at which water is available: shallow W has a shorter lagged effect than deep W, possibly indicative of *Larrea*'s bimodal rooting distribution, the dynamics of root hydraulic recovery and growth, and/or colonization by mycorrhizae. Finally, drivers of Ψ_D differed between control and watered shrubs, highlighting a potential long-term legacy effect of large moisture events on diurnal plant Ψ regulation. This study demonstrates that plant Ψ can be regulated by atmospheric and soil moisture drivers across hourly to seasonal timescales and highlights the importance of including antecedent conditions when quantifying plant responses to environmental conditions.

Acknowledgements

We thank K. Hultine, G. Koch, M. Mack, and three anonymous reviewers for constructive comments on earlier versions of this manuscript. Field data were made available through the efforts of Roberto Fernández, Sarah Bauer, Lisa Stano, Guy Telesnicki, David Tremmel and James Reynolds. The data collection efforts were partially supported by NASA Headquarters under the Earth System Science Fellowship (grant no. NGT5-30355).

Author contributions

K.O. conducted the field study, J.S.G. and K.O. both contributed to the design of the research questions and approaches, J.S.G. performed the data analysis, K.O. supervised the data analysis, J.S.G. led the writing of the manuscript, and K.O. contributed to manuscript writing.

ORCID

Jessica S. Guo http://orcid.org/0000-0002-9566-9182
Kiona Ogle http://orcid.org/0000-0002-0652-8397

References

Anderegg WR, Schwalm C, Biondi F, Camarero JJ, Koch G, Litvak M, Ogle K, Shaw JD, Shevliakova E, Williams A. 2015. Pervasive drought legacies in forest ecosystems and their implications for carbon cycle models. *Science* **349**: 528–532.

Apple ME, Thee CI, Smith-Longozo VL, Cogar CR, Wells CE, Nowak RS. 2005. Arbuscular mycorrhizal colonization of *Larrea tridentata* and *Ambrosia dumosa* roots varies with precipitation and season in the Mojave Desert. *Symbiosis* **39**: 131–135.

Bamberg SA, Kleinkopf GE, Wallace A, Vollmer A. 1975. Comparative photosynthetic production of Mojave Desert shrubs. *Ecology* **56**: 732–736.

Barbour MM, Buckley TN. 2007. The stomatal response to evaporative demand persists at night in *Ricinus communis* plants with high nocturnal conductance. *Plant, Cell & Environment* **30**: 711–721.

BassiriRad H, Tremmel DC, Virginia RA, Reynolds JF, de Soyza AG, Brunell MH. 1999. Short-term patterns in water and nitrogen acquisition by two desert shrubs following a simulated summer rain. *Plant Ecology* **145**: 27–36.

Beatley JC. 1974. Phenological events and their environmental triggers in Mojave Desert ecosystems. *Ecology* **55**: 856–863.

Berger-Landefeldt U. 1936. *Das Wasserhaushalt der Alpenpflanzen.* (Bibliotheca Botanica Vol. 115). Stuttgart, Germany: Schweizerbartsche Verlagsbuchhandlung.

Blackman CJ, Brodribb TJ, Jordan GJ. 2009. Leaf hydraulics and drought stress: response, recovery and survivorship in four woody temperate plant species. *Plant, Cell & Environment* **32**: 1584–1595.

Briones O, Montaña C, Ezcurra E. 1996. Competition between three Chihuahuan Desert species: evidence from plant size–distance relations and root distribution. *Journal of Vegetation Science* **7**: 453–460.

Brodribb TJ, Cochard H. 2009. Hydraulic failure defines the recovery and point of death in water-stressed conifers. *Plant Physiology* **149**: 575–584.

Bucci SJ, Goldstein G, Meinzer FC, Franco AC, Campanello P, Scholz FG. 2005. Mechanisms contributing to seasonal homeostasis of minimum leaf water potential and predawn disequilibrium between soil and plant water potential in Neotropical savanna trees. *Trees* **19**: 296–304.

Caird MA, Richards JH, Donovan LA. 2007. Nighttime stomatal conductance and transpiration in C_3 and C_4 plants. *Plant Physiology* **143**: 4–10.

Caldwell MM. 1976. Root extension and water absorption. In: Lange OL, Kappen L, Schulze ED, eds. *Water and plant life: problems and modern approaches.* Berlin, Germany: Springer, 63–85.

Castillo VM, Gómez-Plaza A, Martínez-Mena M. 2003. The role of antecedent soil water content in the runoff response of semiarid catchments: a simulation approach. *Journal of Hydrology* **284**: 114–130.

Chaves MM, Flexas J, Pinheiro C. 2009. Photosynthesis under drought and salt stress: regulation mechanisms from whole plant to cell. *Annals of Botany* **103**: 551–560.

Choat B, Jansen S, Brodribb TJ, Cochard H, Delzon S, Bhaskar R, Bucci SJ, Feild TS, Gleason SM, Hacke UG. 2012. Global convergence in the vulnerability of forests to drought. *Nature* **491**: 752–755.

Clark JS. 2005. Why environmental scientists are becoming Bayesians. *Ecology Letters* **8**: 2–14.

Cochard H, Bréda N, Granier A. 1996. Whole tree hydraulic conductance and water loss regulation in *Quercus* during drought: evidence for stomatal control of embolism? *Annals of Forest Science* **53**: 197–206.

Cowan I. 1965. Transport of water in the soil–plant–atmosphere system. *Journal of Applied Ecology* **2**: 221–239.

Cunningham GL, Burk JH. 1973. The effect of carbonate deposition layers ("caliche") on the water status of *Larrea divaricata. American Midland Naturalist* **90**: 474–480.

Damour G, Simonneau T, Cochard H, Urban L. 2010. An overview of models of stomatal conductance at the leaf level. *Plant, Cell & Environment* **33**: 1419–1438.

Dixon HH, Joly J. 1895. On the ascent of sap. *Philosophical Transactions of the Royal Society of London B* **186**: 563–576.

Donovan LA, Linton MJ, Richards JH. 2001. Predawn plant water potential does not necessarily equilibrate with soil water potential under well-watered conditions. *Oecologia* **129**: 328–335.

Donovan LA, Richards JH, Linton MJ. 2003. Magnitude and mechanisms of disequilibrium between predawn plant and soil water potentials. *Ecology* **84**: 463–470.

Doughty CE, Goulden ML, Miller SD, da Rocha HR. 2006. Circadian rhythms constrain leaf and canopy gas exchange in an Amazonian forest. *Geophysical Research Letters* **33**: L15404.

Fernández RJ. 2007. On the frequent lack of response of plants to rainfall events in arid areas. *Journal of Arid Environments* **68**: 688–691.

Fisher JB, Baldocchi DD, Misson L, Dawson TE, Goldstein AH. 2007. What the towers don't see at night: nocturnal sap flow in trees and shrubs at two AmeriFlux sites in California. *Tree Physiology* **27**: 597–610.

Flexas J, Barón M, Bota J, Ducruet J-M, Gallé A, Galmés J, Jiménez M, Pou A, Ribas-Carbó M, Sajnani C *et al.* 2009. Photosynthesis limitations during water stress acclimation and recovery in the drought-adapted *Vitis* hybrid Richter-110 (*V. berlandieri*× *V. rupestris*). *Journal of Experimental Botany* **60**: 2361–2377.

Forster MA. 2014. How significant is nocturnal sap flow? *Tree Physiology* **34**: 757–765.

Franco AC, Soyza AG, Virginia RA, Reynolds JF, Whitford WG. 1994. Effects of plant size and water relations on gas exchange and growth of the desert shrub *Larrea tridentata*. *Oecologia* **97**: 171–178.

Gallé A, Feller U. 2007. Changes of photosynthetic traits in beech saplings (*Fagus sylvatica*) under severe drought stress and during recovery. *Physiologia Plantarum* **131**: 412–421.

Garcia-Forner N, Adams HD, Sevanto S, Collins AD, Dickman LT, Hudson PJ, Zeppel MJB, Jenkins MW, Powers H, Martínez-Vilalta J *et al.* 2016. Responses of two semiarid conifer tree species to reduced precipitation and warming reveal new perspectives for stomatal regulation. *Plant, Cell & Environment* **39**: 38–49.

Garfin G, Jardine A, Merideth R, Black M, LeRoy S. 2013. *Assessment of climate change in the southwest United States: a report prepared for the National Climate Assessment*. Washington, DC, USA: Island Press.

Gelman A, Carlin JB, Stern HS, Rubin DB. 2014. *Bayesian data analysis*. Boca Raton, FL, USA: Taylor & Francis.

Gelman A, Rubin DB. 1992. Inference from iterative simulation using multiple sequences. *Statistical Science* **7**: 457–472.

Goldstein AH, Hultman NE, Fracheboud JM, Bauer MR, Panek JA, Xu M, Qi Y, Guenther AB, Baugh W. 2000. Effects of climate variability on the carbon dioxide, water, and sensible heat fluxes above a ponderosa pine plantation in the Sierra Nevada (CA). *Agricultural and Forest Meteorology* **101**: 113–129.

Greenland S. 2000. Principles of multilevel modelling. *International Journal of Epidemiology* **29**: 158–167.

Hacke UG, Stiller V, Sperry JS, Pittermann J, McCulloh KA. 2001. Cavitation fatigue embolism and refilling cycles can weaken the cavitation resistance of xylem. *Plant Physiology* **125**: 779–786.

Hennessey TL, Field CB. 1991. Circadian rhythms in photosynthesis. *Oscillations in Carbon Assimilation and Stomatal Conductance Under Constant Conditions* **96**: 831–836.

Hinckley TM, Duhme F, Hinckley AR, Richter H. 1983. Drought relations of shrub species: assessment of the mechanisms of drought resistance. *Oecologia* **59**: 344–350.

Hochberg U, Rockwell FE, Holbrook NM, Cochard H. 2018. Iso/anisohydry: a plant–environment interaction rather than a simple hydraulic trait. *Trends in Plant Science* **23**: 112–120.

Hölttä T, Mencuccini M, Nikinmaa E. 2009. Linking phloem function to structure: analysis with a coupled xylem–phloem transport model. *Journal of Theoretical Biology* **259**: 325–337.

Hultine KR, Koepke DF, Pockman WT, Fravolini A, Sperry JS, Williams DG. 2006. Influence of soil texture on hydraulic properties and water relations of a dominant warm-desert phreatophyte. *Tree Physiology* **26**: 313–323.

Ikegami K, Okamoto M, Seo M, Koshiba T. 2009. Activation of abscisic acid biosynthesis in the leaves of *Arabidopsis thaliana* in response to water deficit. *Journal of Plant Research* **122**: 235–243.

Jarvis PG. 1976. The interpretation of the variations in leaf water potential and stomatal conductance found in canopies in the field. *Philosophical Transactions of the Royal Society of London. Series B: Biological Sciences* **273**: 593–610.

Jones HG. 1998. Stomatal control of photosynthesis and transpiration. *Journal of Experimental Botany* **49**: 387–398.

Jones HG, Sutherland RA. 1991. Stomatal control of xylem embolism. *Plant, Cell & Environment* **14**: 607–612.

Kidron GJ. 2009. The effect of shrub canopy upon surface temperatures and evaporation in the Negev Desert. *Earth Surface Processes and Landforms* **34**: 123–132.

Klein T. 2014. The variability of stomatal sensitivity to leaf water potential across tree species indicates a continuum between isohydric and anisohydric behaviours. *Functional Ecology* **28**: 1313–1320.

Kropp H, Loranty M, Alexander HD, Berner LT, Natali SM, Spawn SA. 2017. Environmental constraints on transpiration and stomatal conductance in a Siberian Arctic boreal forest. *Journal of Geophysical Research: Biogeosciences* **122**: 487–497.

Kutsch WL, Herbst M, Vanselow R, Hummelshøj P, Jensen NO, Kappen L. 2001. Stomatal acclimation influences water and carbon fluxes of a beech canopy in northern Germany. *Basic and Applied Ecology* **2**: 265–281.

Lange OL, Tenhunen JD, Braun M. 1982. Midday stomatal closure in Mediterranean type sclerophylls under simulated habitat conditions in an environmental chamber: I. Comparison of the behaviour of various European Mediterranean species. *Flora* **172**: 563–579.

Larter M, Brodribb TJ, Pfautsch S, Burlett R, Cochard H, Delzon S. 2015. Extreme aridity pushes trees to their physical limits. *Plant Physiology* **168**: 804–807.

Lauenroth WK, Sala OE, Milchunas DG, Lathrop RW. 1987. Root dynamics of *Bouteloua gracilis* during short-term recovery from drought. *Functional Ecology* **1**: 117–124.

Lo Gullo MA, Nardini A, Salleo S, Tyree MT. 1998. Changes in root hydraulic conductance (K_R) of *Olea oleaster* seedlings following drought stress and irrigation. *New Phytologist* **140**: 25–31.

Loik ME, Breshears DD, Lauenroth WK, Belnap J. 2004. A multi-scale perspective of water pulses in dryland ecosystems: climatology and ecohydrology of the western USA. *Oecologia* **141**: 269–281.

Ludlow M, Fisher M, Wilson J. 1985. Stomatal adjustment to water deficits in three tropical grasses and a tropical legume grown in controlled conditions and in the field. *Functional Plant Biology* **12**: 131–149.

Lunt OR, Letey J, Clark SB. 1973. Oxygen requirements for root growth in three species of desert shrubs. *Ecology* **54**: 1356–1362.

Maherali H, Pockman WT, Jackson RB. 2004. Adaptive variation in the vulnerability of woody plants to xylem cavitation. *Ecology* **85**: 2184–2199.

Manzi M, Lado J, Rodrigo MJ, Zacarías L, Arbona V, Gómez-Cadenas A. 2015. Root ABA accumulation in long-term water-stressed plants is sustained by hormone transport from aerial organs. *Plant and Cell Physiology* **56**: 2457–2466.

Martínez-Vilalta J, Garcia-Forner N. 2017. Water potential regulation, stomatal behaviour and hydraulic transport under drought: deconstructing the iso/anisohydric concept. *Plant, Cell & Environment* **40**: 962–976.

Martínez-Vilalta J, Poyatos R, Aguadé D, Retana J, Mencuccini M. 2014. A new look at water transport regulation in plants. *New Phytologist* **204**: 105–115.

McAdam SAM, Brodribb TJ, Ross JJ. 2016. Shoot-derived abscisic acid promotes root growth. *Plant, Cell & Environment* **39**: 652–659.

McDowell NG, Fisher RA, Xu C, Domec JC, Hölttä T, Mackay DS, Sperry JS, Boutz A, Dickman L, Gehres N *et al.* 2013. Evaluating theories of drought-induced vegetation mortality using a multimodel–experiment framework. *New Phytologist* **200**: 304–321.

Meinzer FC, Hinckley TM, Ceulemans R. 1997. Apparent responses of stomata to transpiration and humidity in a hybrid poplar canopy. *Plant, Cell & Environment* **20**: 1301–1308.

Mencuccini M, Hölttä T. 2010. The significance of phloem transport for the speed with which canopy photosynthesis and belowground respiration are linked. *New Phytologist* **185**: 189–203.

Mencuccini M, Mambelli S, Comstock J. 2000. Stomatal responsiveness to leaf water status in common bean (*Phaseolus vulgaris* L.) is a function of time of day. *Plant, Cell & Environment* **23**: 1109–1118.

Mitchell PJ, McAdam SAM, Pinkard EA, Brodribb TJ. 2017. Significant contribution from foliage-derived ABA in regulating gas exchange in *Pinus radiata*. *Tree Physiology* **37**: 236–245.

Montaña C, Cavagnaro B, Briones O. 1995. Soil water use by co-existing shrubs and grasses in the southern Chihuahuan Desert, Mexico. *Journal of Arid Environments* **31**: 1–13.

Monteith JL, Unsworth MH. 1990. *Principles of environmental physics*. New York, NY, USA: Edward Arnold.

Mooney HA, Björkman O, Collatz GJ. 1978. Photosynthetic acclimation to temperature in the desert shrub, *Larrea divaricata*: I. Carbon dioxide exchange characteristics of intact leaves. *Plant Physiology* **61**: 406–410.

Naumburg E, Housman DC, Huxman TE, Charlet TN, Loik ME, Smith SD. 2003. Photosynthetic responses of Mojave Desert shrubs to free air CO_2 enrichment are greatest during wet years. *Global Change Biology* **9**: 276–285.

Ng GHC, Bedford DR, Miller DM. 2015. Identifying multiple time scale rainfall controls on Mojave Desert ecohydrology using an integrated data and modeling approach for *Larrea tridentata*. *Water Resources Research* **51**: 3884–3899.

Nilsen ET, Sharifi MR, Rundel PW, Jarrell WM, Virginia RA. 1983. Diurnal and seasonal water relations of the desert phreatophyte *Prosopis glandulosa* (honey mesquite) in the Sonoran Desert of California. *Ecology* **64**: 1381–1393.

North GB, Nobel PS. 1995. Hydraulic conductivity of concentric root tissues of *Agave deserti* Engelm. under wet and drying conditions. *New Phytologist* **130**: 47–57.

Noy-Meir I. 1973. Desert ecosystems: environment and producers. *Annual Review of Ecology and Systematics* **4**: 25–51.

Odening WR, Strain BR, Oechel WC. 1974. The effect of decreasing water potential on net CO_2 exchange of intact desert shrubs. *Ecology* **55**: 1086–1095.

Oechel WC, Strain BR, Odening WR. 1972. Tissue water potential, photosynthesis, C-labeled photosynthate utilization, and growth in the desert shrub *Larrea divaricata* Cav. *Ecological Monographs* **42**: 127–141.

Ogle K, Barber JJ, Barron-Gafford GA, Bentley LP, Young JM, Huxman TE, Loik ME, Tissue DT. 2015. Quantifying ecological memory in plant and ecosystem processes. *Ecology Letters* **18**: 221–235.

Ogle K, Lucas RW, Bentley LP, Cable JM, Barron-Gafford GA, Griffith A, Ignace D, Jenerette GD, Tyler A, Huxman TE *et al.* 2012. Differential daytime and night-time stomatal behavior in plants from North American deserts. *New Phytologist* **194**: 464–476.

Ogle K, Reynolds JF. 2002. Desert dogma revisited: coupling of stomatal conductance and photosynthesis in the desert shrub, *Larrea tridentata*. *Plant, Cell & Environment* **25**: 909–921.

Ogle K, Wolpert RL, Reynolds JF. 2004. Reconstructing plant root area and water uptake profiles. *Ecology* **85**: 1967–1978.

O'Grady A, Eamus D, Hutley L. 1999. Transpiration increases during the dry season: patterns of tree water use in eucalypt open-forests of northern Australia. *Tree Physiology* **19**: 591–597.

Oren R, Sperry JS, Katul GG, Pataki DE, Ewers BE, Phillips N, Schäfer KVR. 1999. Survey and synthesis of intra- and interspecific variation in stomatal sensitivity to vapour pressure deficit. *Plant, Cell & Environment* **22**: 1515–1526.

Pfautsch S, Adams MA. 2013. Water flux of *Eucalyptus regnans*: defying summer drought and a record heatwave in 2009. *Oecologia* **172**: 317–326.

Plummer M. 2003. JAGS: a program for analysis of Bayesian graphical models using Gibbs sampling. Proceedings of the 3rd international workshop on distributed statistical computing: Vienna 125.

Plummer M. 2013. rjags: Bayesian graphical models using MCMC. R package version 3.

Plummer M, Best N, Cowles K, Vines K. 2006. CODA: convergence diagnosis and output analysis for MCMC. *R News* **6**: 7–11.

Pockman WT, Sperry JS. 2000. Vulnerability to xylem cavitation and the distribution of Sonoran Desert vegetation. *American Journal of Botany* **87**: 1287–1299.

Prein AF, Holland GJ, Rasmussen RM, Clark MP, Tye MR. 2016. Running dry: the U.S. Southwest's drift into a drier climate state. *Geophysical Research Letters* **43**: 1272–1279.

R Core Team. 2016. *R: a language and environment for statistical computing*. Vienna, Austria: R Foundation for Statistical Computing.

Raftery AE, Lewis SM. 1992. Comment: one long run with diagnostics: implementation strategies for Markov chain Monte Carlo. *Statistical Science* **7**: 493–497.

Resco de Dios V, Gessler A, Ferrio JP, Alday JG, Bahn M, del Castillo J, Devidal S, García-Muñoz S, Kayler Z, Landais D *et al.* 2016. Circadian rhythms have significant effects on leaf-to-canopy scale gas exchange under field conditions. *GigaScience* **5**: e43.

Resco V, Ignace DD, Sun W, Huxman TE, Weltzin JF, Williams DG. 2008. Chlorophyll fluorescence, predawn water potential and photosynthesis in precipitation pulse-driven ecosystems – implications for ecological studies. *Functional Ecology* **22**: 479–483.

Rigby JR, Porporato A. 2006. Simplified stochastic soil-moisture models: a look at infiltration. *Hydrology and Earth System Sciences Discussions* **10**: 861–871.

Runyon EH. 1936. Ratio of water content to dry weight in leaves of the creosote bush. *Botanical Gazette* **97**: 518–553.

Ryan EM, Ogle K, Zelikova TJ, LeCain DR, Williams DG, Morgan JA, Pendall E. 2015. Antecedent moisture and temperature conditions modulate the response of ecosystem respiration to elevated CO_2 and warming. *Global Change Biology* **21**: 2588–2602.

Sala O, Lauenroth W. 1982. Small rainfall events: an ecological role in semiarid regions. *Oecologia* **53**: 301–304.

Sala OE, Lauenroth WK, Parton WJ. 1992. Long-term soil water dynamics in the shortgrass steppe. *Ecology* **73**: 1175–1181.

Scanlon BR. 1994. Water and heat fluxes in desert soils: 1. Field studies. *Water Resources Research* **30**: 709–719.

Scholander PF, Hammel H, Bradstreet ED, Hemmingsen E. 1965. Sap pressure in vascular plants. *Science* **148**: 339–346.

Schulze E-D, Lange OL, Evenari M, Kappen L, Buschbom U. 1974. The role of air humidity and leaf temperature in controlling stomatal resistance of *Prunus armeniaca* L. under desert conditions. *Oecologia* **17**: 159–170.

Schwalm CR, Anderegg WRL, Michalak AM, Fisher JB, Biondi F, Koch G, Litvak M, Ogle K, Shaw JD, Wolf A *et al.* 2017. Global patterns of drought recovery. *Nature* **548**: 202.

Seager R, Ting M, Held I, Kushnir Y, Lu J, Vecchi G, Huang H-P, Harnik N, Leetmaa A, Lau N-C *et al.* 2007. Model projections of an imminent transition to a more arid climate in southwestern North America. *Science* **316**: 1181–1184.

Sellin A. 1999. Does pre-dawn water potential reflect conditions of equilibrium in plant and soil water status? *Acta Oecologica* **20**: 51–59.

Shen W, Jenerette GD, Hui D, Scott RL. 2016. Precipitation legacy effects on dryland ecosystem carbon fluxes: direction, magnitude and biogeochemical carryovers. *Biogeosciences* **13**: 425–439.

Skelton RP, West AG, Dawson TE. 2015. Predicting plant vulnerability to drought in biodiverse regions using functional traits. *Proceedings of the National Academy of Sciences, USA* **112**: 5744–5749.

Smith SD, Monson R, Anderson JE. 1997. *Physiological ecology of North American desert plants*. New York, NY, USA: Springer Science & Business Media.

Sperry J, Hacke U, Oren R, Comstock J. 2002. Water deficits and hydraulic limits to leaf water supply. *Plant, Cell & Environment* **25**: 251–263.

Sperry JS, Love DM. 2015. What plant hydraulics can tell us about responses to climate-change droughts. *New Phytologist* **207**: 14–27.

Sperry JS, Wang Y, Wolfe BT, Mackay DS, Anderegg WRL, McDowell NG, Pockman WT. 2016. Pragmatic hydraulic theory predicts stomatal responses to climatic water deficits. *New Phytologist* **212**: 577–589.

Spiegelhalter DJ, Best NG, Carlin BP, Linde AVD. 2002. Bayesian measures of model complexity and fit. *Journal of the Royal Statistical Society: Series B (Statistical Methodology)* **64**: 583–639.

Syvertsen JP, Cunningham GL, Feather TV. 1975. Anomalous diurnal patterns of stem xylem water potentials in *Larrea tridentata*. *Ecology* **56**: 1423–1428.

Tardieu F, Davies WJ. 1992. Stomatal response to abscisic acid is a function of current plant water status. *Plant Physiology* **98**: 540–545.

Tardieu F, Simonneau T. 1998. Variability among species of stomatal control under fluctuating soil water status and evaporative demand: modelling isohydric and anisohydric behaviours. *Journal of Experimental Botany* **49**: 419–432.

Tenhunen JD, Lange OL, Jahner D. 1982. The control by atmospheric factors and water stress of midday stomatal closure in *Arbutus unedo* growing in a natural macchia. *Oecologia* **55**: 165–169.

Titus JH, Titus PJ, Nowak RS, Smith SD. 2002. Arbuscular mycorrhizae of Mojave Desert plants. *Western North American Naturalist* **62**: 327–334.

Urli M, Porté AJ, Cochard H, Guengant Y, Burlett R, Delzon S. 2013. Xylem embolism threshold for catastrophic hydraulic failure in angiosperm trees. *Tree Physiology* **33**: 672–683.

Virlouvet L, Fromm M. 2015. Physiological and transcriptional memory in guard cells during repetitive dehydration stress. *New Phytologist* **205**: 596–607.

Wilkinson S, Davies WJ. 2002. ABA-based chemical signalling: the co-ordination of responses to stress in plants. *Plant, Cell & Environment* **25**: 195–210.

Williams AP, Allen CD, Macalady AK, Griffin D, Woodhouse CA, Meko DM, Swetnam TW, Rauscher SA, Seager R, Grissino-Mayer HD *et al.* 2013. Temperature as a potent driver of regional forest drought stress and tree mortality. *Nature Climate Change* **3**: 292–297.

Xu Z, Zhou G, Shimizu H. 2009. Are plant growth and photosynthesis limited by pre-drought following rewatering in grass? *Journal of Experimental Botany* **60**: 3737–3749.

Yan S, Wan C, Sosebee RE, Wester DB, Fish EB, Zartman RE. 2000. Responses of photosynthesis and water relations to rainfall in the desert shrub creosote bush (*Larrea tridentata*) as influenced by municipal biosolids. *Journal of Arid Environments* **46**: 397–412.

Zhang Q, Manzoni S, Katul G, Porporato A, Yang D. 2014. The hysteretic evapotranspiration–vapor pressure deficit relation. *Journal of Geophysical Research: Biogeosciences* **119**: 125–140.

Supporting Information

Additional Supporting Information may be found online in the Supporting Information tab for this article:

Fig. S1 Site- and shrub-level environmental conditions, including maximum daily D, soil moisture from 0–30 cm and 30–60 cm, and moisture inputs (precipitation and irrigation).

Fig. S2 Model fit of observed vs predicted Ψ_B and Ψ_D for individual measurements.

Fig. S3 Model fit of observed vs predicted Ψ_B and Ψ_D averaged across all shrubs for each round of measurement.

Fig. S4 Estimates of the intercepts of the Ψ_B and Ψ_D models, representing the expected Ψ_B and Ψ_D at mean or nominal conditions.

Fig. S5 Interaction plots of the significant interactions in the Ψ_D model.

Methods S1 Priors for the Ψ_B and Ψ_D models.

Methods S2 Description of Ψ_B and Ψ_D models without lagged effects.

Notes S1 Data for the Ψ_B and Ψ_D models.

Notes S2 JAGS code for the Ψ_B model.

Notes S3 JAGS code for the Ψ_D model.